



# A novel non-ionic surfactant extract derived from *Chromolaena odorata* as shale inhibitor in water based drilling mud



Wilberforce Nkrumah Aggrey<sup>a,b,\*</sup>, Nana Yaw Asiedu<sup>c</sup>, Caspar Daniel Adenutsi<sup>d,e</sup>, Prosper Anumah<sup>f</sup>

<sup>a</sup> Department of Petroleum Engineering, Kwame Nkrumah University of Science and Technology, Kumasi, PMB, Ghana

<sup>b</sup> Petroleum Research Laboratories-Drilling Fluids Engineering, Kwame Nkrumah University of Science and Technology, Kumasi, PMB, Ghana

<sup>c</sup> Department of Chemical Engineering, Kwame Nkrumah University of Science and Technology, Kumasi, PMB, Ghana

<sup>d</sup> School of Energy-Resources, China University of Geosciences, Beijing, 100083, PR China

<sup>e</sup> Beijing Key Laboratory of Unconventional Natural Gas, Geology Evaluation and Development Engineering, Beijing, 100083, PR China

<sup>f</sup> Department of Energy and Environmental Engineering, University of Energy and Natural Resource, Ghana

## ARTICLE INFO

### Keywords:

Chemical engineering  
Physical chemistry  
Organic chemistry  
Natural product chemistry  
Materials chemistry  
Analytical chemistry

## ABSTRACT

High performance clay swelling inhibitors play a vital role in improving inhibition characteristics of shales. The linkages between the inhibition's characteristics of the non-ionic surfactant extract from bio-based inhibitors are yet to be fully explored in the literature. This paper reports the use of a crude extract containing saponins from *Chromolaena odorata* (CO) leaf, which act as surfactants for inhibiting shale hydration. Determination of the inhibitive property of nonionic surfactant was made through measurements of surface-active properties, inhibition tests, filtration, rheological and strength test.

The experimental findings on CO showed that it was highly compatible and very stable with conventional water-based drilling fluids (WBDFs), a highly effective shale inhibitor and a works through plugging and viscosity acting effect in the shale system.

## 1. Introduction

Among the many complications and challenges encountered during drilling operations, well stability remains one of the most difficult challenges. In drilling mud engineering there is increasing research into more usable, environmentally friendly water base muds. These muds are deployed to meet economic, technical and legal issues related to environmentally sensitive areas around the globe (Bol et al., 1994; Maulana et al., 2018; Asadi et al., 2018; Al-saba et al., 2018; Kumar et al., 2018; Lim et al., 2018; L. J. Hall et al., 2018; Meng et al., 2012; Tayab et al., 2018; An and Yu, 2018). It is reported in the literature concerning instability challenges in the wellbore that shales (making up more than 75% of drilled formations) are the major cause of over 90% of wellbore-stability problems (Kang et al., 2016; Zhuang et al., 2017; Steiger and Leung, 1992; Zeynali, 2012; Cheatham, 1984; Ji and Geehan, 2013; Lu, 1988; Oort, 2003). This is due to clay-rich shales dominant constituent in the formation (75%) been drilled. Numerous studies reports also on the challenge of designing low cost biodegradable environmentally friendly drilling fluid system capable of improving/curbing

well instability issues (An and Yu, 2018; Razali et al., 2018).

Dehghanpour et al., (2012) reported the relationship between swelling and dispersion properties of reactive clays. As the drilling section enters the shale zones, water-sensitive rock (shale) swells due to the adsorption of water leading to the reduction in compressive strength deformation due to indentation hardness and other operational challenges (O'Brien and Chenevert, 1973; Lomba et al., 2000). In many wellbores, such issues have led to abandoning the wells completely. Shale-fluid interaction has been extensively investigated with the general understanding that wellbore stability in shale is to a large extent affected by the type of mud (Fritz, 1986; Müller-Vonmoos and Løken, 1989; Lal, 1999). Generally, formation instability problems stem from mechanical, physical and chemical effects (Zeynali, 2012; Lal, 1999).

Oil based drilling fluids (OBDF) over the last three decades have seen a wide use of its application in inhibition of shale swelling. They were the drilling fluids of choice but their high cost and damage to the environment have limited its use and attention has shifted to WBDFs through the deliberate enhancement by shale inhibitors (Tambach et al., 2004; Pruett, 1987; Patel et al., 2007; Blachier et al., 2009). The most widely

\* Corresponding author.

E-mail addresses: [wnaggrey@yahoo.com](mailto:wnaggrey@yahoo.com), [wnaggrey.coe@knust.edu.gh](mailto:wnaggrey.coe@knust.edu.gh) (W.N. Aggrey).

used shale inhibitor is Potassium Chloride (KCl) due to the small size of its cation and hydration energy (Pruett, 1987). However, it has several disadvantages which is of concern to the immediate surroundings of drilling operations resulting in high cost of disposal (Patel et al., 2007).

Alternatives for oil-based muds with the following characteristics; additive compatibility, environmental compliance, ease of engineering and cost for effective deployment in water-based drilling fluids are in high demand. Most shale inhibitors currently in use are inorganic based and very few studies on the bio-based materials are available in the literature. However, studies have reported the likely occurrence of saponins in over 400 plant species (Ribeiro et al., 2013). These saponins have varied structural diversity in the class of compounds due primarily to the structures of the aglycone (Ribeiro et al., 2013; Bani and Le Gall, 1992) and are responsible for the surfactant acting characteristics of bio-surfactants. Chemically, saponins structures involve a polar part and a non-polar part which is responsible for their surface-active properties (Phan et al., 2001).

Non-ionic surfactants can adsorb onto surfaces of hydrated expandable clay due to their silanol groups as well as the negative surface ( $-ve$ ) charges of the clay. This process results in suppressing the clay hydration. Previous studies have looked at possible plants that could be used in shale inhibition process. However, none so far to the best of our knowledge have looked at deployment of these synthesized saponin non-ionic WBDF effect on the linkages between the inhibition characteristics of the non-ionic surfactants, the stability, strength and particle bridging characteristics on actual field shale samples.

Extensive study of various ionic compounds and ionic surfactants in inhibiting shale swelling has been conducted with little research into the potential of natural surfactants in the mitigation of shale hydration and swelling. A search for viable natural surfactants to inhibit shale hydration is of keen interest due to its low cost, low environmental footprints and availability.

In this paper, leaf extracts of CO, a herbaceous perennial (Ngozi Igboh et al., 2009) very rich in saponins (non-ionic surfactant), readily available in many parts of the world, easily synthesized, biodegradable and utilized in many countries for treatment of fresh cuts and burns (Phan et al., 2001; Ngozi Igboh et al., 2009) is synthesized for the inhibition of shale during drilling operations. To the best of our knowledge, this paper is the first in studying the inhibition and stability activity characteristics of bio-based crude extract (non-ionic surfactant) in the hope of addressing the gaps existing in literature on non-ionic surfactant application in water-based drilling fluids (WBDFs) studies. This paper reports test on uniaxial compressive strength, microscopy study and Fourier transform infra-red test analysis in addition to the standard inhibition tests used in evaluation of the crude leaf extract from CO in WBDFs and their influence on shale inhibition.

## 2. Materials & methods

### 2.1. Sampling, extraction and characterization

CO leaves, Fig. 1a, were picked from the Awomaso Farms-Kumasi, Ghana. Table 1 gives some properties of CO. In this study, the spray drying method for converting a crude mixture in the liquid form to powder is employed (C. W. Hall, 1988; American Petroleum Institute, 1995). A Lab Plant SD-05 Spray Dryer (Labplant, UK) was utilized in the spray dryer method as shown in Fig. 1b.

### 2.2. Shale mineral characterization

Two shale cores, Shale-1 and Shale-2 sourced from 7700.18 ft. - 7768.41 ft. depth and 5456.4ft-5459.1 ft. depth respectively were received and kept at room temperature and pressure from the Ghana National Petroleum Corporation. Each shale core received was divided into five parts using a mineral oil and the core cutter for easy utilization in inhibition analysis. Using a KA-210 gas permeameter (Coretest, USA)

the klinkenberg permeability for shale-1 and shale-2 cores were determined to be 0.09 mD-0.12 mD and 1.45 mD-4.47 mD respectively. The cation exchange capacity was found to be 24–35, 12–15 and 62 meq/100 g for the shale-1, shale-2 and Na-bentonite respectively using the methylene blue test according to API 13B-1.

Mineral compositions of cores were conducted using Empyrean Diffractometer Pan Analytical D5000. The operational conditions were 40 mA, 40 kV and employed a Co  $K\alpha$  radiation. Scanning of shale samples was made at 30–80 ( $2\theta$ ) and step size of 0.021°. The X-ray diffraction for the shale mineral compositions of cores and sodium bentonite determined by XRD analysis is presented in Table 2.

### 2.3. Drilling fluid composition

The drilling fluids made for the test were named, deionized water (DI), KCl and CO mud. The compositions were same except the inhibitor used i.e. water, KCl and CO. The common additives in all three mud configurations were 100 g/L NaCl, 22.5 g/L starch, 6.85 g/L PAC-LV and 3 g/L xanthan gum. For example, a DI mud formulation involves DI, 100 g/L NaCl, 22.5 g/L starch, 6.85 g/L PAC-LV and 3 g/L xanthan gum. A KCl mud formulation involved KCl, 100 g/L NaCl, 22.5 g/L starch, 6.85 g/L PAC-LV and 3 g/L xanthan gum and CO mud formulation involved CO, 100 g/L NaCl, 22.5 g/L starch, 6.85 g/L PAC-LV and 3 g/L xanthan gum. However, in the test whenever a special formulation is made for a specific protocol, it would be explicitly stated. It should be stated that water is not a shale inhibitor, but the formulation is made as a control to compare the case where inhibitors are deployed to the case where they are not. It should also be noted that unless it is stated, all mud compositions used followed section 2.3 mud compositions.

### 2.4. Measurements of surface-active properties

Three properties were measured to study the surface-active nature of the non-ionic surfactant. First was the critical micelle concentration (CMC). There are different methods for CMC determination (Moslemizadeh et al., 2017a). The method of conductivity was used in CMC measurements according to experimental standard reference NSRDS-NBS 36. A high master concentration solution was made. This was carried out by homogeneously adding powdered *Chromolaena odorata* to de-ionized water. Simultaneously the mixture was stirred via the Stuart magnetic hot-plate stirrer for 2hrs. In all cases of lower *Chromolaena odorata* concentrations de-ionized water was used to dilute the master concentration to the required concentration. Oakion Con 700 Benchtop was employed in measurements of pH and Conductivity. Finally, the CMC of the *Chromolaena odorata* was obtained. This was carried out by a plot of conductivity and pH against relevant *Chromolaena odorata* concentrations. The concentration value read at the point where the two concentration straight line of the curve meets (i.e. point of inflection) corresponds to the CMC.

The second surface-active property studied was the adsorption characteristics of the CO. A conductivity technique was used for the adsorption test using different concentrations of the CO. In this test, adsorption of CO on the pulverized shale is measured by calculating the concentration of CO in water prior to and after the CO adsorption by the shale. The quantity of CO adsorption over the tested period on pulverized shale was calculated. Adsorption calculations were evaluated according to a method presented by Moslemizadeh (Moslemizadeh and Shadizadeh, 2017). Aqueous CO solutions of varying concentrations were formulated and conductivity values of the solutions, ( $C_b$ ) were measured using OAKION CON 700 benchtop. A Plot of the conductivity versus concentration was then made for the respective concentrations made. After measurement of 15g of shale powder with high precision Toledo mass balance was made and left in the Memmert Universal oven (UF800-UK) at 120 °C for 2hrs. 50 ml of each CO solution was weighed and recorded as  $m_t$  before 10 g of dried shale powder ( $m_s$ ) was added. The mixture was stirred for 24 hours with the magnetic stirrer to reach equilibrium. Equal



**Fig. 1.** a) *Chromolaena odorata* Leaf Collected for Analysis. b) Lab Plant SD-05 Spray Dryer used for test. c) Malvern Zetasizer Nano ZS90. d) 5-Speed Hot Roller Oven. e) FANN Rheometer model. f) API Low Pressure Multiple Filter Press.

**Table 1**  
Properties of CO.

Product	Total Extracted Powder of CO
Part of Interest	Leaves
Description of Method	Spray Drier/Centrifuge
Final Product	Fine Powder
Colour	Greenish-Brown to Brown
Solubility in -15 °C- Water	Soluble
Solubility in 75 °C- Water	Soluble
Density	0.08 g/cm <sup>3</sup>
Loss on Drying (LOD) at 100 °C after 6 h	1.3–2.1%
Total ash at 500 °C after 4 h	9.8–13%
Applications	Herbal Medicine

**Table 2**  
X-ray diffraction for shale mineral compositions of cores and sodium bentonite determined by XRD analysis.

Minerals	Shale -1 (wt. %)	Shale-2 (wt. %)	Bentonite (%)
Montmorillonite	30.3	-	58
Quartz	5	52.5	17
Albite	-	-	-
illite	24.2	-	3
Kaolinite	18.2	10.9	-
Feldspar	6.1	18.8	-
Cristobalite	-	3	14
Calcite	5.7	-	3
Gypsum	-	-	1
Dolomite	1	-	1
Halite	1	-	-
Anorthite	-	-	3

volume of all the suspensions were poured into separate centrifuge tubes and samples allowed centrifuging for 4 hours at 4500 rpm. After a beaker was used to receive each of the supernatant poured and the conductivity values of these solutions, ( $C_e$ ) measured using OAKION CON 700 benchtop. Finally the amount of CO adsorbed was calculated using the relationship below

$$CO \text{ adsorption, } D = \frac{m_t \times (C_b - C_e)}{m_s} \times 10^{-3} \quad (\text{mg/g} - \text{shale powder})$$

The conductivity techniques employed in the adsorption was done as required of experimental standard reference NSRDS-NBS 36 as already described above.

The third surface-active property studied was the zeta potential of the CO. This was done to explore the trends in stability of the CO as concentration increased or decreased during the drilling process. Zetasizer Nano ZS90 by Malvern instruments (UK) offered zeta potential measurements as shown Fig. 1c. With a standard concentration of the aqueous Na-bentonite (formulated mud) dispersion at 0.5 mass% (i.e. 0.5 % (wt%)) different concentrations of CO were added. The mixture was stirred and shaken with a magnetic stirrer at 200 RPM for 16 h and measurement made of zeta potential at atmospheric conditions using a zeta potential analyzer. This measurement was carried out for all prepared surfactant solutions with concentrations of 0.015wt %, 0.025wt %, 0.035wt %, 0.045wt %, respectively.

## 2.5. Inhibition tests

### 2.5.1. Degree of bentonite hydration

Patel et al., (2007), described a widely accepted methodology of



studying the interaction of Na-bentonite on the rheology of a mud with and without a shale inhibitor. 15 g of commercial bentonite (Na-Bentonite) was used as base formulation clay with various concentrations of CO (solution of inhibitor, 350 ml). The mixture was homogenized with an Ofite Model 9B Five Spindle Mixer and hot rolled in an Ofite 5-roller Oven (an API pressurized cell with a capacity of 500 ml) as shown in Fig. 1d at 95 °C each for 16hrs after which the rheological properties were determined. Continuously, more base formulation clay is added and rolling in the ofite 5-roller oven continued until such a time that it became very thick such that measurements of rheological properties could not be determined. Using a method by Friedheim et al., (2011) employing a Fann Rheometer Model 286 as shown in Fig. 1e rheological measurements were computed using the 300–600 rpm dial readings to obtain inhibition test results. Results for 3.5 mass% potassium chloride were also obtained and compared with results of 3.5 mass% CO concentration.

### 2.5.2. Filtration test

Standard filtration test measurements using formulated 8 mass % Na-bentonite mud was gradually mixed with various CO concentrations (0.5 mass %-4.5 mass %) and dispersions made and thereafter hot rolled at 95 °C for 16hr in an ofite 5 roller-oven. Finally, the filtrate loss was measured using an Ofite Multiple Filter Press stage as shown Fig. 1f according to the API recommended practice (American Petroleum Institute, 1995).

### 2.5.3. Sediment analysis and dispersion studies

A method described by Moslemizadeh (Moslemizadeh et al., 2017a) used to carry out precipitation tests. Here the tendency for Na-bentonite to precipitate when interacting with an inhibitive medium as well as the low tendency towards hydration and swelling was studied.

The evaluation criteria adopted for the dispersion test was reduction in shale cutting volume of the test sample exposed to differing water activity in confined conditions (Israelachvili, 2011). The test procedure described by Shadizadeh (Shadizadeh and Moslemizadeh, 2015a) were utilized in studies of dispersion. 20 g of shale cuttings was dried at 120 °C in the Memmert oven for 2 hrs. Test fluids were then prepared and stirred awaiting addition of shale cuttings. 20g of dried shale cuttings were then added to 350 ml of all test fluids and allowed to hot roll at 120 °C for 16 hours in the roller oven. The remaining cuttings were screened using Retsch sieve mesh. After sieving the remaining cuttings were washed and dried at 120 °C. Finally the retrieved cuttings percentages for all test fluids were obtained.

### 2.5.4. Compatibility test

It is imperative that the CO designed must be compatible with the engineering design with other additives employed in the mud program. In order that the compatibility is found rheological and filtration test of WBDFs are conducted and calculated before and after addition of CO. The results so found are indicative of the mud compatibility of the CO. In carrying out the test 3.5 mass% CO were added to the three specific formulated fluids for this test (Table 3), for 16 h at 120 °C and the samples were aged in the Ofite 5 roller-oven. After the readings of the dial (600rpm and 300rpm) using Fann rheometer model 286 and filter loss using API low pressure multiple filter press, pre and post CO modification are noted, and rheological results calculated by Eqs. (1), (2), and (3). Rheological and filter loss results before the addition of CO is calculated as well as after the addition of CO. These values are then compared to each other. Standard test procedure API 13B-1 (American Petroleum Institute, 1995) was employed.

$$Ap. Vis = \frac{D1}{2} \quad (1)$$

$$Pla. Vis = D1 - D2 \quad (2)$$

$$Yld Pt = D2 - Pla. Vis \quad (3)$$

Where;

Ap. Vis - apparent viscosity (cp) D1 – dial reading at 600  
 Pla. Vis - plastic viscosity (cp) D2 – dial reading at 300  
 Yld Pt – yield point (cp)

## 2.6. Formation strength and interaction test

Uniaxial compressive strength (UCS) tests were conducted on the core samples at ambient and higher temperatures of 120 °C. Drilling fluids are exposed to varying degrees of temperature regimes and hence a simulation study on their performance is critical under higher temperatures.

The strength of the Shales rocks is tested (subjected to a UCS test) before and after contact with the formulated CO, KCl and DI drilling fluids. The composition of the formulated mud for CO, KCl and DI are shown in Table 4. The mud compositions were all same except the inhibitor agent i.e. water, CO and KCl. This gives an indication of the formulated fluid inhibitor contribution towards the total inhibition potential. For ambient temperature test, the sample was soaked in the test sample for 30 days and then after tested. For the higher temperature test the sample was soaked in the tested sample for 30 days and thereafter put in a Memmert universal oven for 4h before UCS was conducted using ELE International rock uniaxial compression strength test machine. UCS measurements were done as required of experimental standard reference ASTM D7012-14e1. The following test procedures were carried out for UCS test at both low and high temperature;

### Low temperature UCS

1. Core samples received were Cut into equal sizes and weighed with mass balance
2. 3500g of testing solutions -aqueous CO solutions of varying concentrations along with a deionized water blank (solution) were Prepared.
3. Each cut core samples were soaked for 29 days in the ready solutions.
4. The breaking strength of both the saturated and the dry cut cores were determined using ELE International rock unconfined compressive strength testing equipment

### High Temperature UCS

5. Steps 1–3 were repeated
6. Sample cores were then removed and placed in oven for 16hrs
7. The breaking strength using ELE International rock uniaxial compression strength test machine were determined and readings noted.

After UCS test, fragments of the crushed samples are imaged using a JEOL 5800 LV scanning electron microscope (SEM).

FTIR studies were conducted on the raw Na-bentonite powder as well as the interaction between the Na-bentonite modified various concentrations of CO and 3.5 mass% KCl. A Prepared dispersions of Na-bentonite in DI were shaken using Stuart magnetic stirrer CD162 for 24

**Table 3**  
Test matrix of specially formulated fluids.

FORMULATED FLUID (FF)	COMPOSITIONS
FF1	Deionised water +50g/LKCl +100g/LNaCl +22.5g/Lstarch +6.85 g/L PAC-LV + 3 g/L XC + 2.5g/LPHPA +3% (vol) Glycol
FF2	Deionised water +50g/LKCl +100g/LNaCl +22.5g/Lstarch +6.85 g/L PAC-LV + 3 g/L XC + 2.5g/LPHPA
FF3	Deionised water +50 g/L KCl +22.5g/Lstarch +6.85 g/L PAC-LV + 3 g/L XC + 45mass% Barite

**Table 4**  
The composition of the formulated mud for CO, KCl and DI for UCS test.

Drilling mud	COMPOSITIONS
DI	+100 g/L NaCl, 22.5 g/L starch, 6.85 g/L PAC-LV and 3 g/L xanthan gum
CO <sup>a</sup>	CO+100 g/L NaCl, 22.5 g/L starch, 6.85 g/L PAC-LV and 3 g/L xanthan gum
KCl	KCl+100 g/L NaCl, 22.5 g/L starch, 6.85 g/L PAC-LV and 3 g/L xanthan gum

<sup>a</sup> Various CO concentration variation made.

h at 29 °C for uniform homogenous mixture to be established.

Dispersions were centrifuged at 4000 rpm for 3 h using a multifuge X3R centrifuge by Thermo Scientific/Heraeus to obtain the sediments which were dried at 120 °C using Memmert universal oven UFE800 for 1 h and then after powdered using agate mortar and pestle. The sample now obtained is ready to undergo FTIR analysis. Same procedure was employed for the CO and KCl formulations to get samples ready for FTIR studies.

FT-IR measurements are employed to understand the complexities of shale surface interaction with the bio-nonionic surfactant (Zhong et al., 2012). 8 g of pulverized shale was measured with a mass balance and dispersed vigorously using the Stuart magnetic stirrer at 20 °C for 2 h at a concentration of 2 mass % in DI. Then after, the sample now well

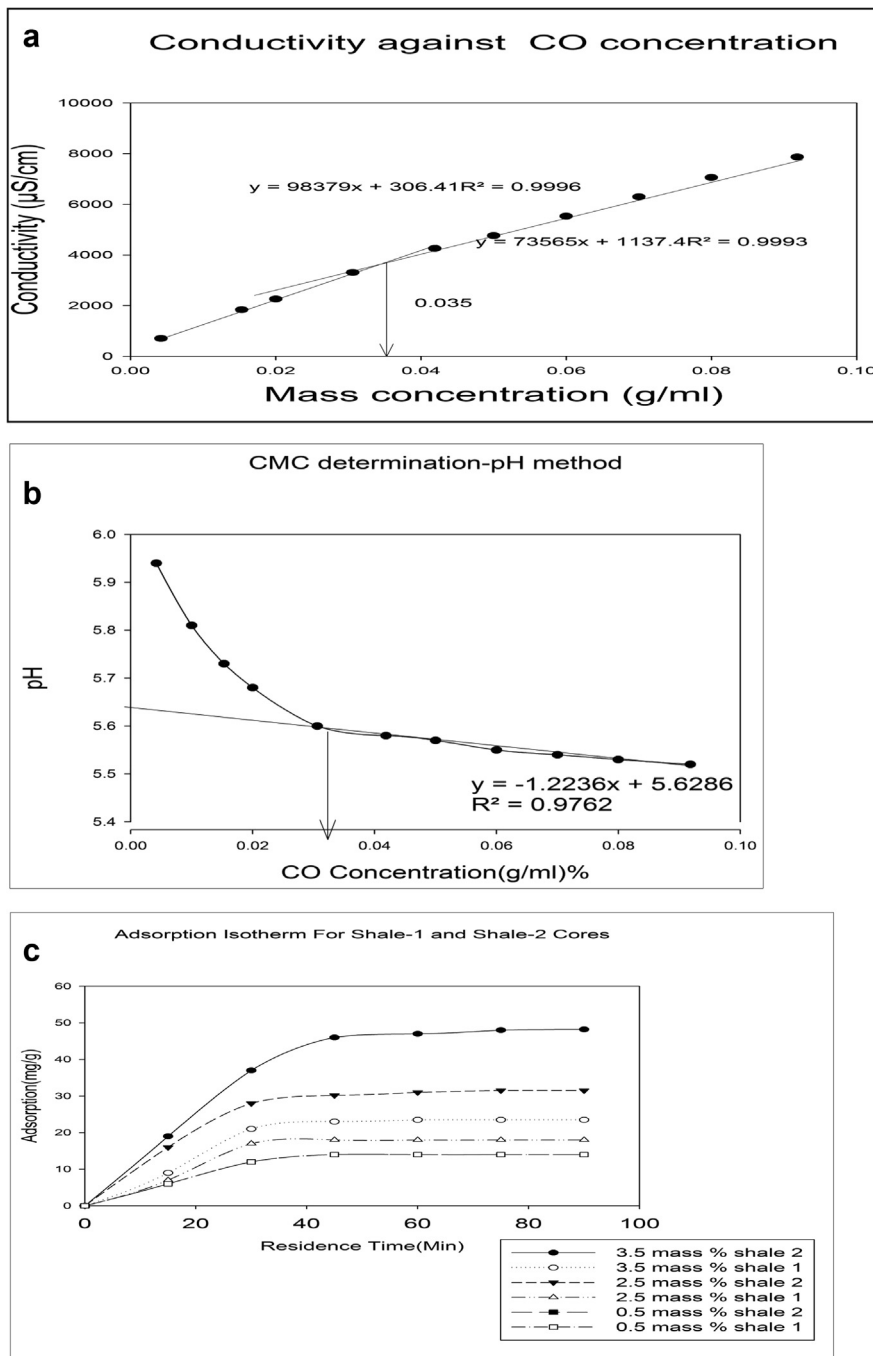


**Fig. 2.** a) Critical micelle Concentration determination using Conductivity Method. b). CMC determination using pH method. c) Adsorption Isotherm of CO on Shale Cores at different concentrations (mass %).

homogenized was left in a tight seal for 16 h. 5 g of CO was then added. Using the Stuart magnetic stirrer, the entire mixture was stirred for 8 h at 20 °C. Using the Thermo Fisher Scientific/Hareaus multifuge X3R centrifuge at 4000 RPM the resulting sediment were collected and dried in a vacuum oven at 90 before pulverized. Compression of pulverized samples into KBr pellets were made for analysis of FT-IR.

FTIR measurements were performed using PerkinElmer Spectrum Two instrument. The ratio of the sample to the spectroscopic grade KBr was approximately 1:10. FTIR spectra were an average of 256 spectra collected at room temperature in the 3500-400  $\text{cm}^{-1}$  range using 4 $\text{cm}^{-1}$  resolution.

### 3. Results & discussion

#### 3.1. Inhibition tests

##### 3.1.1. Bentonite loading inhibition characteristics

Results of the surface-active properties of the CO extract are presented in Figs. 2a, b, c and 3. Fig. 4 present results of the rheological parameters as a function of Na-bentonite loading. When Na-bentonite absorbs water, it swells up rapidly leading to dissociation of the clay's individual unit layers. This results in an increased viscosity of the dispersion. From the results presented in DI, this phenomenon was high, hence the easy adsorption of water leading to an increased resistance to flow as seen from their viscosities. As sodium bentonite concentration increased from 3 mass% to 7.5 mass%, the DI drilling fluid mixture system became very thick and there was no deflection on the dial (Fann rheometer). A higher rheological profile for DI drilling fluid mixture system was subsequently recorded. In surfactant study, CMC is the most critical parameter that helps the optimization of the surfactant and the proper design of the fluid system. The working CMC value calculated from the average of the conductivity and pH methods employed as shown in Fig 2a and b was 3.5%.

##### 3.1.2. Surface inhibitive characteristics

Above the CMC, the effective significant inhibitive property of CO reduces even as concentration keeps increasing due to the formation of micelles. In strong inhibitive systems, there is a rapid change in rheological lines in various fluid mixture concentrations of the Na-bentonite. From Fig. 4, the gaps between the rheological lines enlarge from the beginning as CO concentration increased. It narrowed however after the system approached the CO CMC indicating the relationship between inhibition strength of CO to its concentration. Above the CMC, it was clear from the result presented that there was not much increase in the inhibitive potential of the CO. The maximum loaded Na-bentonite for 3.5 mass% was found to be 30 mass% CO. This was consistent with the Na-bentonite adsorption density (Fig. 2c) which increased from 1.1 mg/g to

46.98 mg/g when initial CO concentrations was 0.5 mass% to a maximum CO concentration of 4.0 mass% for shale-1 adsorption and 0.5 mass% to 3.5 mass% for shale-2. Secondly the relationship between adsorption rate and mineralogy for shale-1 and shale-2 was evident. In KCl for shale inhibition, the max amount of loaded Na-bentonite for 3.5 mass% KCl was 27.5 mass%. This result indicates the potential of the novel crude extract non-ionic surfactant, CO compared with KCl.

##### 3.1.3. Fluid loss inhibitive characteristics

The high-performance CO extract was also observed in the filtration test results shown in Fig. 5. Formulation 1 (Na-bentonite in de-ionized water) produced the lesser amount of filtration when analyzed than formulation 2 (CO formulations). The different working mechanism i.e. effect of water and CO on clay. Clays have peculiar outstretched level surface-platey shape like nature, small particle size and high capacity of expansion of montmorillonite.

It is also conclusive that adsorption also played a role. It was observed that the adsorption was a function of the clay content of the shale. That may be as a result of clay content differences with the two shales and the rock properties (Table 2). Higher amounts of smectites suggest higher affinity for water adsorption. XRD analysis (Table 2) indicated that shale-1 was abundant in smectite than shale-2 making it more wetting in character hence a greater degree of adsorption which influences the filtration characteristics. Within 30min of the test, 14.6 ml filtrate volume was recorded. However, CO yield increased with concentration i. e mass% formulations of 0.5, 1.5, 2.5, 3.5 and 4.5 yielded 20 ml, 24 ml, 28 ml, 34 ml and 38 ml fluid loss respectively.

The main reasons for the high fluid loss result by the CO can be attributable to the concept of particle delamination due to the change in clay particles and the hydration capacities of the clay (Moslemizadeh et al., 2017a). This process occurs when expandable clays imbibe water resulting in high particle liberation, rapid development of a watertight filter cake and small API fluid-loss value. The concept of particle delamination could also be thought of as the action of the non-ionic surfactant influence on the flow characteristics of montmorillonite by their effect on the card-house networks of the clays and by the electro viscous effect. This is characterised by the information on surface potential, double-layer structure colloid characteristics, and point of zero charge which from observation made by the measurements of zeta potential the presence of CO on the clay surfaces affects the structure of the electric double layer which changes the zeta potential for different levels of concentration applied. Stability in colloidal dispersions was measured in the high zeta potential of the clay dispersions. Hence the higher the zeta potential the more stable the dispersions are as compared with lower zeta potential. Low zeta potential dispersions tend to coagulate and thus a measure of these phenomena helps find out the stability of the dispersions. From the results in Fig. 3, the de-ionized water-dispersions

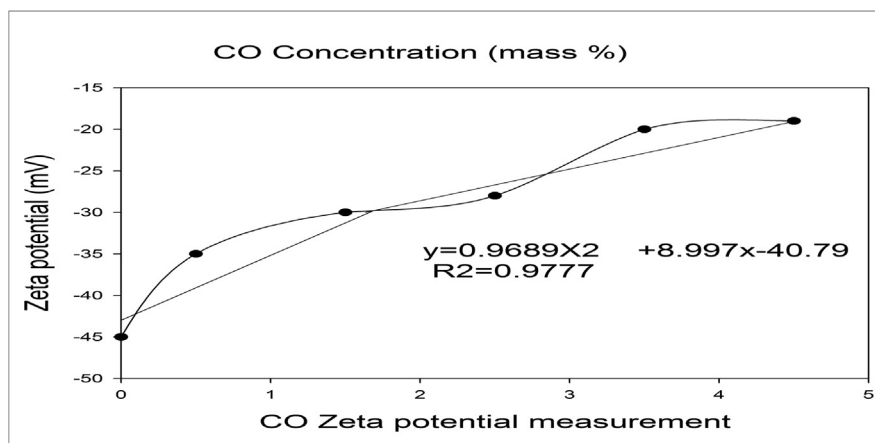


Fig. 3. Zeta Measurements of CO Concentrations.

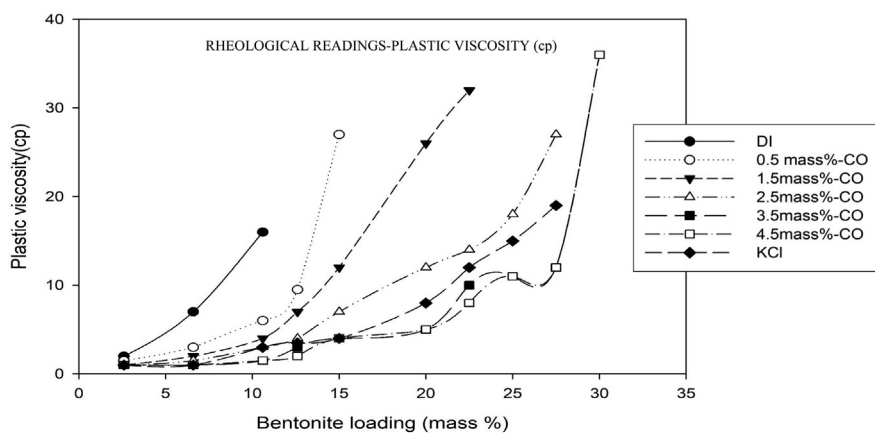


Fig. 4. Inhibition tests of CO (Rheological Readings –Plastic Viscosity (cP)).

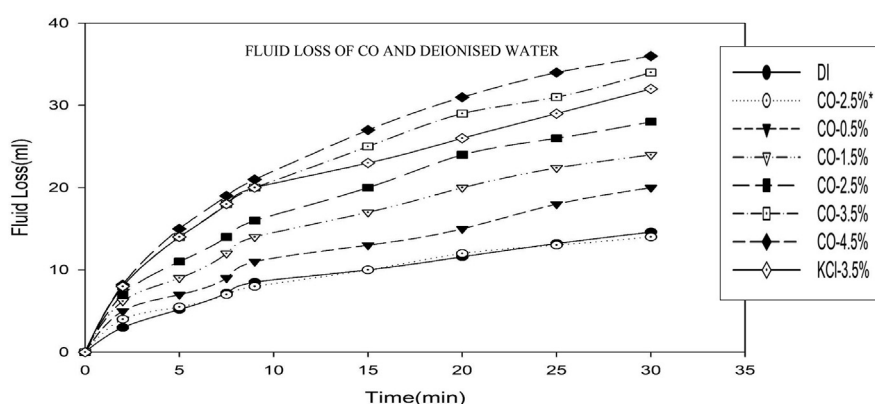


Fig. 5. Filtration (Fluid Loss) for CO, KCl and De-Ionised Water (DI).

shows a high zeta potential reading of 41.5 whereas the readings for increasing CO concentration reduced from 35.3–19.23 for concentrations of 0.5%–4.5 % respectively. These results meant that the CO had reduced appreciably the clay surface affinity to the water molecules and successfully impeded clay hydration hence the main reasons for the high fluid loss result by the CO. From the results, KCl generated filtration volumes of 25 ml at 30 mins as compared to the formulation 2 (CO systems) which recorded 54ml for concentrations 2.5%. Again, it shows the superior inhibitive characteristic of the CO to impede the hydration and expansion potential of Na-bentonite. The bentonite mass was doubled for 2.5% CO formulation and the results (Fig. 5) were the same for the DI. The result indicated that it was possible to inhibit the formation without impeding on rheological characteristics.

### 3.1.4. Sedimentation –dispersion inhibitive characteristics

Comparing the inhibitive flocculation of bentonite, CO and KCl as presented in the sedimentation results in Fig. 6, it shows that when bentonite was used without CO and KCl, the particles of bentonite absorb water excellently in the de-ionized water. This led to the generation of a stable well hydrated colloidal dispersion. However, in the presence of CO there was flocculation of the bentonite particles to form sediments. Increases in the concentration of the CO led to greater flocculation and a faster rate of settling of the particles at the bottom which led to formation of denser sediments. This phenomenon also occurred when the KCl was used as the inhibition agent. CO has a superior inhibition potential as compared to KCl. The degree of stable dispersion is a function of Na-bentonites high water adsorption and expansion capacity. Results of DI showed a firm uniform formation of stable dispersion consistent with theory whereas that containing 3.5 mass% CO produced sediment. Notice was made of the correlation between the CO concentration and

the dispersion stability formed. Within the first two days CO concentration of 0.5%–4.5% showed reduction in the h/H ratio to around 0.34–0.421 respectively. No noticeable change was observed after this period. This was also consistent with the theory that the inhibition of CO increases with increasing concentration up until the CMC was reached.

Dispersion tests results are presented in Fig. 7. In DI the rate of recovery is 25% (Fig. 7), representing a high adsorption of water and dispersion of the shale. With the interaction of CO and KCl, readings of 41.5 %–59.5 % and 54.15 % were recorded respectively. This result was indicative of the greater inhibition and dispersion degree of CO to hydration of shale cuttings than the more traditional KCl. The fluid formulation readings (formulation 1 (FF1), fluid formulation (FF2) and fluid formulation 3 (FF3)) when CO was deployed with other additive mixtures shown in Fig. 7 on various WBDFs interaction of shale-1 and shale-2 were in the ranges of 77.5%–91.8% and 65.6%–79.8% for shale-1 and shale-2 respectively.

These results again affirmed the inhibitive nature/potential of CO and its performance when deployed in WBDFs. It was observed that shale recovery was a function of the CO concentration and shale mineralogy. This result meant the hydration and expansion ability of shale decreases with increase in CO. Shale-1 formulations contained high levels of smectites evidenced in SEM results shown in Fig. 8 a-f and thus they held the highest propensity to swell compared to those of shale-2 as shown in Fig. 8 g-i with no smectites and thus they held the lowest propensity to swell. This literally means that they as well have the highest degree of change in hydration influence. Shale-1 results responded with the highest recovery rate. The contribution of CO to the hydration could be credited to the repulsion due to hydration as a result of the swelling shale as shown in Fig. 8 a-f.

This resultant action by the CO must be effectual on the strength of

## SEDIMENTATION TEST ANALYSIS OF CO/KCl

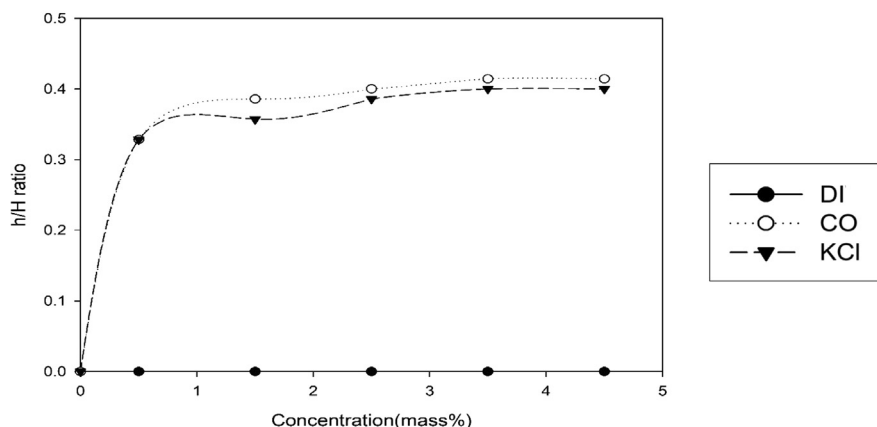


Fig. 6. Sedimentation test of CO, KCl and De-ionised Water (DI).

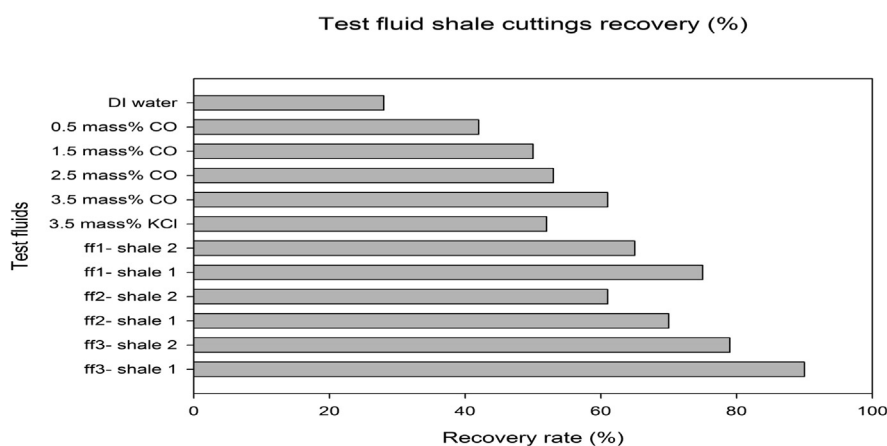


Fig. 7. Dispersion Analysis Test for CO on Bentonite Clay and Formulated Fluids on Shale-1 and Shale-2. \*Test on 0.5-3.5 mass% CO and 3.5 mass% KCl were conducted on Shale-1.

the shale it interacts with due to the contribution of CO to the hydration. This was seen in the uniaxial compressive strength (UCS) test (Fig. 9). UCS of shale-1 sample prior to been soaked with CO was 52213.58 psi. DI mud decreased the UCS of shale core to 31908.3 psi at ambient temperatures and 17404.53 psi at 120 °C. KCl mud increased the UCS of shale to 40511.94 psi at ambient temperatures and 27155.41 psi at 120 °C. CO mud formulations from 0.5%-3.5% increased the UCS at ambient temperatures to 34649.53 psi-42234.99 psi respectively. At 120 °C UCS for the CO mud formulations increased from 20305.28 psi to 35435.62 psi.

From the SEM at 120 °C of the samples shown in Fig. 8 it can be evidenced that the shale particles are broader and less disperse than at the lower ambient (25 °C) temperature. Dispersion is a function of the shale's permeability and particle interaction bonding. The images give a clue as to the competencies of the CO interaction with the shale compared to KCl and the UCS confirms this interaction as temperature increases. We also glean the effect of the amount of clay in the shale and their UCS. The shale with the high smectite portion compacted more than that with kaolinite. Clearly there exist from UCS results a relationship between increasing temperature and the strength of the shale using crude non-ionic surfactants extract.

The inhibition potential of the CO clearly shows that it increases with temperature and relates to the mineralogy and clay amount in the shale from the XRD.

### 3.2. Compatibility analysis

Analysis of the CO effect on the drilling fluid was favorable as result of compatibility test showed. For incompatibility of the CO with the test fluids huge fluctuations in the measured data of the test done for pre and post modification of the fluid should be observed. The expected results should be close to unity for the fluid to be deemed compatible and when it is far more than 1 then it means the measure of compatibility is low. All results presented in Table 5 are close to one (1) which was indicative of the insignificant effect CO had on the rheological properties of the mud. With less fluctuation in research data recorded it can be concluded therefore that the CO was highly compatible with common WBDFs additives.

### 3.3. FTIR inference into mechanics and mechanism of inhibition

Fig. 10 presents the infrared-spectra of unmodified and modified montmorillonite with CO and KCl. That of the unmodified montmorillonite exhibited the characteristics of smectite clay. After adsorption of CO onto montmorillonite some changes were observed. The insert table in Fig. 10 shows the before and after characteristics of the major changes occurring. In the modified-montmorillonite, the band at 2923.55  $\text{cm}^{-1}$  and 2358.98  $\text{cm}^{-1}$  was absent. Notice was observed of wearing out of a shoulder peak at 1112  $\text{cm}^{-1}$  which correlate with the bending vibration of the bond axis joining silicon and oxygen atoms (Si-O-Si). From the observations in FTIR, it can be argued that CO decreases the absorbed



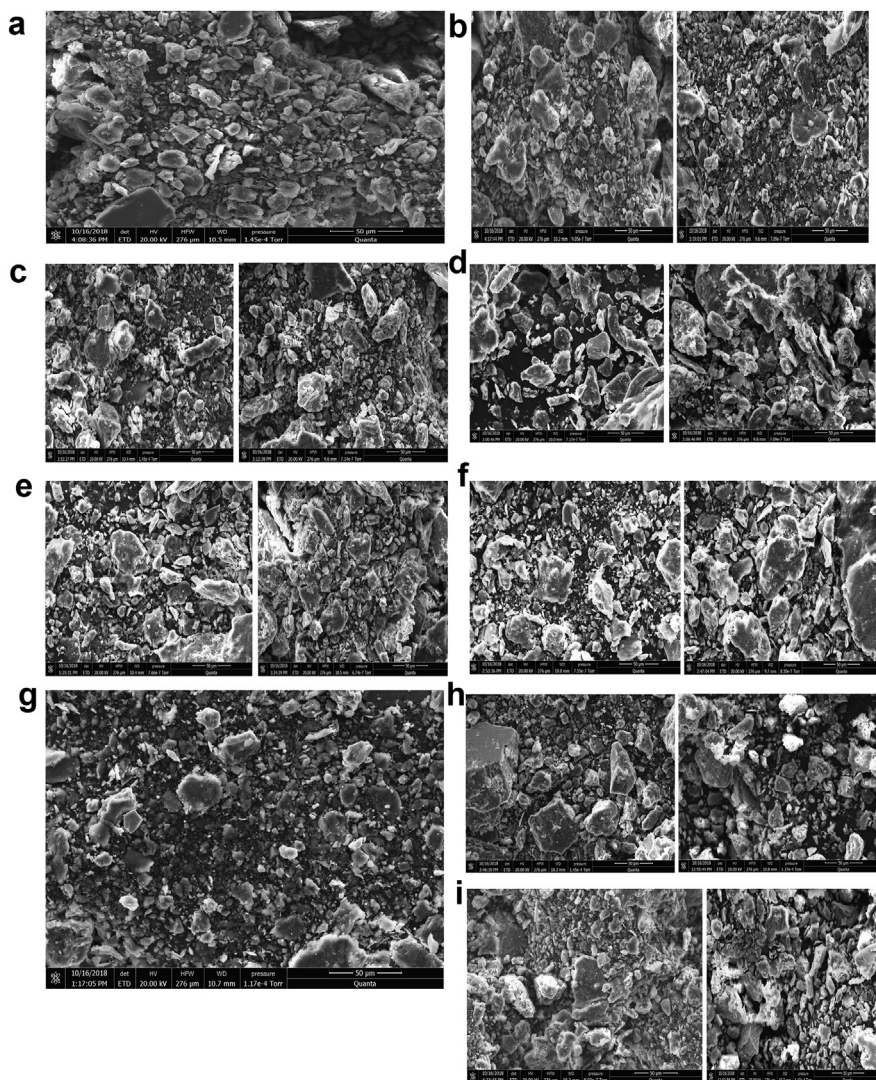


**Fig. 8.** a) SEM for raw shale1 –Sample Uncontaminated with mud formulation. b) (1) SEM for 3.5 mass % CO @ Ambient (25°C) on Shale-1 (2) SEM for 3.5 mass % KCl @ Ambient (25°C) on Shale-1. c) (1) SEM for 3.5 mass % CO @ 80°C on Shale-1 (2) SEM for 3.5 mass % KCl @ 80°C on Shale-1. d) (1) SEM for 3.5 mass % CO @120°C on Shale-1 (2) SEM for 3.5 mass % KCl @ 120°C on Shale-1. e) (1) SEM for 0.5 mass % CO @ 25 °C on Shale-1 (2) SEM for 1.5 mass % CO @ 25 °C on Shale-1. f) (1) SEM for 2.5 mass % CO @ 25 °C on Shale-1 (2) SEM for 3.5 mass % CO @ 25°C on Shale-1. g) SEM for raw shale 2 – sample uncontaminated with mud formulations. h) (1) SEM for 3.5 mass % CO @ 80 °C on Shale-2 (2) SEM for 3.5 mass % KCl @ 80°C on Shale-2. i) (1) SEM for 3.5 mass % CO @ 120 °C on Shale-2 (2) SEM for 3.5 mass % KCl @ 120°C on Shale-2.

UCS Test for shale-1 with various formulations

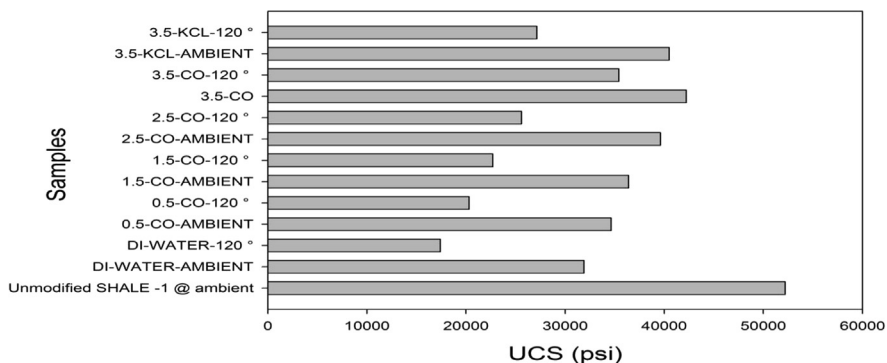


**Fig. 9.** Uniaxial compressive strength (UCS) test for shale-1.

water by montmorillonite physically, through adsorption. This process occurs via the hydrogen bond linking the hydrophilic units of the CO to the free oxygen atoms on siloxane plane.

When CO extracts encounter water-sensitive shales, due to competition with water molecules to absorb on shale surfaces via hydrogen bonds

operating between OH<sup>-</sup> groups of CO and free oxygen atoms on silica plane of clays (montmorillonite) in the shales, the net result is a decrease in accessible sites for the molecules of water.

With WBDFs the action of water and ions alters the condition of the shale stress via alterations in the formations pore pressure and the

**Table 5**  
Measurements of compatibility of CO with additives.

Formulation	PV	G.S	A.V	Y.P	F.L	MD	MCT
A (FF With CO)/(FF Without CO)	0.913043	0.927273	0.871795	0.8904	0.916667	1	0.97561
% Decrease	0.086957	0.072727	0.128205	0.1096	0.083333	0	0.02439
B (FF With CO)/(FF Without CO)	0.823529	0.89	0.816327	0.934659	0.906542	1	0.930233
% Decrease	0.176471	0.11	0.183673	0.065341	0.093458	0	0.069767
C (FF With CO)/(FF Without CO)	0.903226	0.955587	0.921569	0.956522	0.993684	1	1
% Decrease	0.096774	0.044413	0.078431	0.043478	0.006316	0	0

A- 3.5mass% CO + F1.

B- 3.5mass% CO + F2.

C- 3.5mass% CO + F3.

MCT-mud cake thickness.

PV-plastic viscosity.

G.S-gel strength.

A.V-apparent viscosity.

Y.P-yield point.

F.L-fluid loss.

MD-mud density.

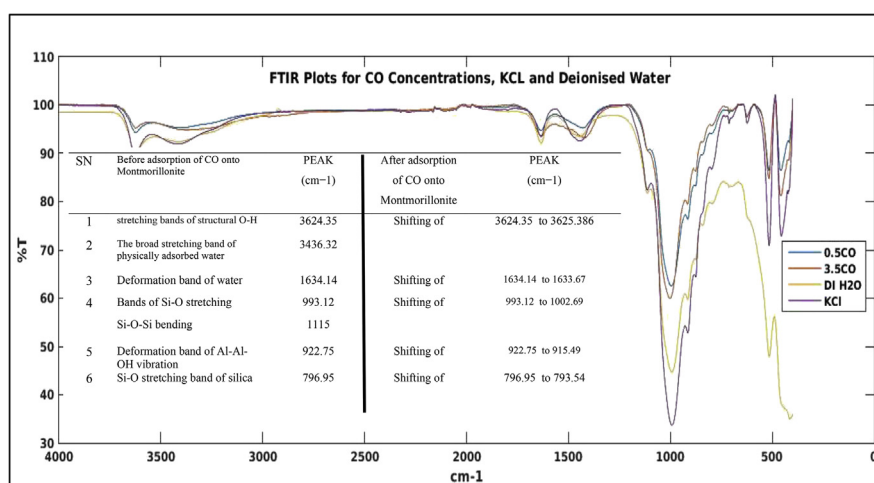


**Fig. 10.** FTIR Spectrum Graph Results for CO Concentrations, KCL and Deionised Water (DI H<sub>2</sub>O).

strength of the shale. The hydration or de-hydration of the shale pattern then results in formation of swelling stresses. These consequently results in wellbore instability depending on the degree of the ion and water influx.

The hydrogen bonding to areas on exposed clays leads to shale membrane development. This probably disallows the solute from entering the pores due to solute - pore size ratio increment. These actions lead to reduced permeability and contaminant reduction in the internal pore structural dimensions. This process makes the environment of the CO in terms of wetting characteristics less wetting. The ability of CO to engulf the clay platelets renders the clay more hydrophobic. This hydrophobicity delivered by the CO is sustained as far as there is enough of the CO to engulf the clay platelets. The degree of shale permeability (as in this case shale-2) influences the extent at which CO wins the adsorption “war” with the water. The higher the permeability, the lower the margin of win and vice versa. In high permeability shale, CO has less time to stick to the pores and arrange itself in a tight strong aggregate whereas in tight formations CO is able. With each buildup of the mud interaction with the shale there occur a series of stacking of the short-chain CO of low molecular weight particles until a dynamic shale pore size remains. This stacking slows fluid movement through the shale pore permeability matrix resulting in plugging and viscosity combined effect.

It can be said from the FTIR and SEM analysis earlier presented that CO helps improve the inhibitive potential of shales and their improvement characteristics is based on the plugging and viscosity combined effect principle. This occurs due to absorption of CO on shale via

hydrogen bonds operating between OH<sup>-</sup> groups of CO and free oxygen atoms on silica plane of clays (montmorillonite) in the shales.

### 3.4. Cost and environmental considerations

Two key design considerations worthy of note are the cost of the formulated mud and the environmental considerations. CO is abundant and grows in the wild. It has high volumes of saponins hence on the case of commerciality, CO is very scalable, and extraction is fairly easy. As a natural crude extract containing saponins CO does not pose any serious environmental challenge/risk. Compared to the other shale inhibitors in use in industry now, its high availability, compatibility, extractability, operability and low cost could be considered as factors of interest.

## 4. Conclusions

The research concluded on the following;

1. CO crude extract containing saponins degree of inhibition is comparable to industrial KCl in all inhibition characteristics.
2. UCS established a relationship between increasing temperature and the strength of the shale using crude non-ionic surfactants extract.
3. SEM results validated the functional relationship between temperature and inhibition of crude non-ionic surfactants extract muds. As

temperature increases the inhibition composition i.e. the strength of the shale due to the inhibition of the crude extract increased.

- Concentration range of 2.5–3.5 mass% - CO could be introduced as inhibitor component in WBDFs with a CMC of 3.5 mass% as an optimum concentration to improve the inhibitive characteristics.
- CO crude extract was highly compatible when used alongside the conventional WBDFs additives and also offered stability to Na-bentonite particles in CO aqueous solution
- CO crude extract is easily extractable at minimum cost and readily available as a substitute for commercial KCl.

## Declarations

### Author contribution statement

Wilberforce N. Aggrey: Conceived and designed the experiments; Performed the experiments; Wrote the paper.

Nana Y. Asiedu, Caspar D. Adentusi: Analyzed and interpreted the data; Contributed reagents, materials, analysis tools or data.

Prosper Anumah: Performed the experiments.

### Funding statement

This research did not receive any specific grant from funding agencies in the public, commercial, or not-for-profit sectors.

### Competing interest statement

The authors declare no conflict of interest.

### Additional information

No additional information is available for this paper.

## Nomenclature

API	American Petroleum Institute
CO	<i>Chromolaena odorata</i>
CMC	Critical micelle concentration
DI	Deionized water
FTIR	Fourier transform infrared spectroscopy
SI	Ionic selectivity
% (W/V)	Mass percentage (Mass%)
ME	Membrane Efficiency
mD	Millidarcy
OBDF	Oil based drilling fluid
KCl	Potassium chloride
Na-bentonite	Sodium bentonite
UCS	Uniaxial compressive strength
WBDF	Water based drilling Fluid
WBDFs	Water based drilling Fluids

## References

- Al-saba, M.T., Amadi, K.W., Al-Hadramy, K.O., Al Dushaishi, M.F., Al-Hameedi, A., Alkinani, H., 2018. Experimental investigation of bio-degradable environmental friendly drilling fluid additives generated from waste. In: SPE International Conference and Exhibition on Health, Safety, Security, Environment, and Social Responsibility.
- American Petroleum Institute, 1995. Recommended Practice for Laboratory Testing of Drilling Fluids, fifth ed. [http://ballots.api.org/ecs/sc13/API\\_RP13B-1\\_5Ed\\_TestingWBDF\\_4316.pdf](http://ballots.api.org/ecs/sc13/API_RP13B-1_5Ed_TestingWBDF_4316.pdf).
- An, Yuxiu, Yu, Peizhi, 2018. A strong inhibition of polyethyleneimine as shale inhibitor in drilling fluid. *J. Pet. Sci. Eng.* 161, 1–8 (November 2017). Elsevier Ltd.
- Asadi, M.S., Rahman, K., Hughes, Baker, Company, G.E., Ho Chi, Q D Ta, Ha, V., 2018. "OTC-28421-MS Mitigating Wellbore Stability Challenges of Extended-Reach Drilling in Overpressure and Naturally Fractured Formations Field of Study," No. Lcm.
- Bani, G., Le Gall, P., 1992. "Chromolaena Odorata (L.) R.M. King and H. Robinson in the Congo," No. Bani 1990, pp. 25–28.

- Blachier, C., Michot, L., Bihannic, I., Barrès, O., Jacquet, A., Mosquet, M., 2009. Adsorption of polyamine on clay minerals. *J. Colloid Interface Sci.* 336 (2), 599–606. Elsevier Inc.
- Bol, G.M., Wong, S.-W., Davidson, C.J., Woodland, D.C., 1994. Borehole stability in shales. *SPE Drill. Complet.* 9 (2), 87–94.
- Cheatham, J.B., 1984. Wellbore stability. *SPE J.* 889–896.
- Dehghanpour, H., Zubair, H.A., Chhabra, A., Ullah, A., 2012. Liquid intake of organic shales. *Energy Fuels* 26 (9), 5750–5758.
- Friedheim, J., Guo, Q., Young, S., Gomez, S., 2011. Testing and evaluation techniques for drilling fluids-shale interaction and shale stability. In: 45th U.S. Rock Mechanics/Geomechanics Symposium, 26–29 June, San Francisco, California, vol. 11. American Rock Mechanics Association, San Francisco, CA. <https://www.onepetro.org/conference-paper/ARMA-11-502>.
- Fritz, Steven J., 1986. Ideality of clay membranes in osmotic processes: a review. *Clay Clay Miner.* 34 (2), 214–223.
- Hall, Carl W., 1988. Handbook of industrial drying. *Dry. Technol.* 6 (3), 571–573.
- Hall, Lee J., Deville, Jay P., Santos, Catherine M., Orlando, J Rojas, Salas Araujo, Carlos, 2018. Nanocellulose and biopolymer blends for high-performance water-based drilling fluids. In: IADC/SPE Drilling Conference and Exhibition.
- Israelachvili, Jacob, 2011. Intermolecular and Surface Forces.
- Ji, Lujun, Geehan, Tomas, 2013. "Shale Failure Around Hydraulic Fractures in Water Fracturing of Gas Shale" 2040, pp. 5–7. November.
- Kang, Yili, She, Jiping, Zhang, Hao, You, Lijun, Song, Minggu, 2016. Strengthening shale wellbore with silica nanoparticles drilling fluid. *Petroleum* 2 (2). Elsevier Ltd: 189–95.
- Kumar, Rajeev, Al Busaidi, Salim, Ali, Maayouf, Dhafiyar, Al, Al Amri, Aryaf, Jonathan, S., 2018. SPE/IADC-189357-MS Wellbore Stability and Hole Cleaning Management for Successful Well Design Optimization in Deep Tight Gas Field Concept of Wellbore Stability Analysis.
- Lal, Manohar, 1999. Shale stability: drilling fluid interaction and shale strength. In: SPE Asia Pacific Oil and Gas Conference and Exhibition.
- Lim, Serena, Shell, Mds, Delina, Lyon, Shell Oil Co, Graham Whale, and Shell International, 2018. OTC-28289-MS Drilling Fluid Impact Studies Show that Worker Health and the Environment Can Be Protected while Improving Drilling Performance.
- Lomba, Rosana F.T., Chenevert, M.E., Sharma, Mukul M., 2000. The ion-selective membrane behavior of native shales. *J. Pet. Sci. Eng.* 25 (1–2), 9–23.
- Lu, Cheng-Fa, 1988. A new technique for the evaluation of shale stability in the presence of polymeric drilling fluid. *SPE Prod. Eng.* 3 (03), 366–374.
- Maulana, Herry, Murphy, Oil, Ghosh, Amitava, Baker, Hughes-a, Company, G.E., Paimin, M Razali, Abiabhar, M., 2018. OTC-28249-MS optimizing pore pressure prediction and wellbore stability in drilling ultra deepwater exploration well. In: Offshore Technology Conference Asia, pp. 1–18.
- Meng, Xianghai, Zhang, Yihe, Zhou, Fengshan, Chu, Paul K., 2012. Effects of carbon ash on rheological properties of water-based drilling fluids. *J. Pet. Sci. Eng.* 100, 1–8. Elsevier.
- Moslemizadeh, Aghil, Aghdam, Saeed Khezloo-ye, Shahbazi, Khalil, Zendejboudi, Sohrab, 2017a. A triterpenoid saponin as an environmental friendly and biodegradable clay swelling inhibitor. *J. Mol. Liq.* 247, 269–280. Elsevier B.V.
- Moslemizadeh, Aghil, Shadizadeh, Seyed Reza, 2017. A natural dye in water-based drilling fluids: swelling inhibitive characteristic and side effects. *Petroleum* 3 (3). Elsevier Ltd: 355–66.
- Müller-Vonmoos, Max, Løken, Tor, 1989. The shearing behaviour of clays. *Appl. Clay Sci.* 4 (2), 125–141.
- Ngozi Igboh, M., Jude Ikewuci, C., Catherine Ikewuchi, C., 2009. Chemical profile of *Chromolaena odorata* L. (King and Robinson) Leaves. *Pakistan J. Nutr.*
- O'Brien, Dennis E., Chenevert, Martin E., 1973. Stabilizing sensitive shales with inhibited, potassium-based drilling fluids. *J. Pet. Technol.* 1089–1100.
- Oort, Eric van, 2003. On the physical and chemical stability of shales. *J. Pet. Sci. Eng.* 38 (3–4), 213–235.
- Patel, Arvind, Stamatakis, Stamatakis, Young, Steve, Friedheim, Jim, 2007. "Advances in inhibitive water-based drilling fluids—can they replace oil-based muds?." In: International Symposium on Oilfield Chemistry.
- Phan, T.T., Wang, L., See, P., Grayer, R.J., Chan, S.Y., Lee, S.T., 2001. Phenolic compounds of *Chromolaena odorata* protect cultured skin cells from oxidative damage: implication for cutaneous wound healing. *Biol. Pharm. Bull.* 24 (12), 1373–1379.
- Pruett, J.O., 1987. A potassium-base derivative of humic acid proves effective in minimizing wellbore enlargement in the ventura basin. In: SPE/IADC Drilling Conference.
- Razali, S.Z., Yunus, R., Abdul Rashid, Suraya, Lim, H.N., Mohamed Jan, B., 2018. Review of biodegradable synthetic-based drilling fluid: progression, performance and future prospect. *Renew. Sustain. Energy Rev.* 90 (March). Elsevier Ltd: 171–86.
- Ribeiro, Bernardo Dias, Alviano, Daniela Sales, Barreto, Daniel Weingart, Coelho, Maria Alice Zarur, 2013. Functional properties of saponins from sisal (agave sisalana) and juá (ziziphus joazeiro): critical micellar concentration, antioxidant and antimicrobial activities. *Colloid. Surf. Physicochem. Eng. Asp.* 436. Elsevier B.V.: 736–43.
- Shadizadeh, Seyed Reza, Moslemizadeh, Aghil, Dezaki, Abbas Shirmardi, 2015a. A novel nonionic surfactant for inhibiting shale hydration. *Appl. Clay Sci.* 118, 74–86. Elsevier B.V.
- Steiger, Ronald P., Leung, Peter K., 1992. Quantitative determination of the mechanical properties of shales. *SPE Drill. Eng.* 7 (03), 181–185.
- Tambach, Tim J., Hensen, Emiel J.M., Smit, Berend, 2004. Molecular simulations of swelling clay minerals. *J. Phys. Chem. B* 108 (23), 7586–7596.

Tayab, Muhammad R., Kashwani, Ghanim, Dewi, Novita Sandra, Abou Ali, Etehad, Mohammed, Tariq Hasan, Alhammami, Mohamed Awadh, 2018. SPE-190609-MS an Integrated Approach to Manage Drilling Waste to Minimise Environmental Impacts.

Zeynali, Mohammad Ebrahim, 2012. Mechanical and physico-chemical aspects of wellbore stability during drilling operations. J. Pet. Sci. Eng. 82–83. Elsevier B.V.: 120–24.

Zhong, Hanyi, Qiu, Zhengsong, Huang, Weian, Cao, Jie, 2012. Poly (Oxypropylene)-Amidoamine modified bentonite as potential shale inhibitor in water-based drilling fluids. Appl. Clay Sci. 67–68. Elsevier B.V.: 36–43.

Zhuang, Guanzheng, Zhang, Haixu, Wu, Hao, Zhang, Zepeng, Liao, Libing, 2017. “Influence of the surfactants’ nature on the structure and rheology of organo-montmorillonite in oil-based drilling fluids. Appl. Clay Sci. 135, 244–252.